Shahid Bahonar University of Kerman
Agricultural Biotechnology Journal
Iranian Biotechnology Society
Print ISSN: 2228-6705 Online ISSN: 2228-6500

# Application of staphyloxanthin-silver nanoparticles combination as a sustainable therapeutic platform with anticancer potential

**Hawraa Kareem Judi**
Corresponding Author, Department of Microbiology, College of Veterinary Medicine, University of Al-Qadisiyah, Al- Qadisiyah, Iraq. E-mail: hawraa-kareemjudi@gmail.com

**Hassan Hachim Naser**
Zoonotic Disease Research Unit, College of Veterinary Medicine, University of Al-Qadisiyah, Al- Qadisiyah, Iraq. E-mail: hassan-naser@qu.edu.iq

## *Abstract*

**Objective**

*Staphylococcus aureus* is a major human pathogen that causes a wide range of infections, from minor skin diseases to severe systemic diseases. A golden carotenoid pigment called staphyloxanthin determines the virulence of Staphylococcus aureus. It acts as an antioxidant and protects the bacteria from oxidative stress. The aim of this study was to investigate the molecular and biochemical properties of staphyloxanthin, as well as its role and potential in combination with biogenic silver nanoparticles (AgNPs) for sustained therapy and to evaluate its anticancer activity.

**Materials and methods**

Staphyloxanthin production by clinical isolates of *Staphylococcus aureus* was investigated based on the amount of pigment produced. PCR was used to genetically confirm the biosynthetic genes *crtO, crtP, crtQ, crtM* and *crtN*. Pigment purification was performed using high-performance liquid chromatography (HPLC). Then, DPPH radical scavenging assay was used to investigate its antioxidant capacity. S. aureus extracts were used to synthesize biogenic silver nanoparticles. Surface plasmon resonance peak was confirmed by UV-visible spectroscopy at 425 nm. Then, the cytotoxic and synergistic effects of staphyloxanthin and silver nanoparticles, both individually and in combination, were evaluated against HeLa (cervical) and MCF-7 (breast) cancer cell lines. CHO cells were used as non-cancerous control.

**Results**

Intense golden pigments were observed in seventy-five percent of the isolates. All staphyloxanthin biosynthesis genes were confirmed by PCR. A single, well-defined peak (retention time: 8.12-8.23 min; area: 639,700.9-28035.9 mA h) was detected by HPLC. The strong antioxidant activity of this pigment resulted in 86% of DPPH radicals being scavenged at a concentration of 320 µg/mL. This activity is at the level and magnitude of the activity of ascorbic acid. The concentration of spherical biogenic silver nanoparticles (23.06-40.12 nm) was 55.6 ± 2.1 µg/mL. Superior dose-dependent cytotoxicity against cancer cells was achieved by the staphyloxanthin-AgNP combination treatment, providing complete inhibition at a concentration of 320 µg/mL while maintaining low toxicity to CHO cells. Combination index values (CI < 1) confirmed strong synergy, increasing the potency of the individual treatments by 2.1- to 3.5-fold.

**Conclusions**

According to the results obtained, it can be said that the staphyloxanthin-silver nanoparticle (STX-AgNP) complex can act as a promising and multifunctional therapeutic platform with potent and selective anticancer activity. Given its strong synergistic effects and biogenic origin, it can be envisaged to have potential applications in the sustainable treatment of cancer and the management of antimicrobial resistance. However, further studies on a larger scale are needed to draw definitive conclusions.

**Keywords:** Anticancer activity, silver nanoparticles, *Staphylococcus aureus*, Staphyloxanthin

**Paper Type:** Research Paper.

**Citation:** Judi, H. K., & Naser, H. H. (2025). Application of staphyloxanthin-silver nanoparticles combination as a sustainable therapeutic platform with anticancer potential. *Agricultural Biotechnology Journal,* 17(4), 415-438.

---

*Agricultural Biotechnology Journal,* 17(4), 415-438. DOI: 10.22103/jab.2025.25829.1760

Received: September 10, 2025. Received in revised form: November 07, 2025.

Accepted: November 08, 2025. Published online: November 30, 2025.

Publisher: Shahid Bahonar University of Kerman & Iranian Biotechnology Society.



---

## Introduction

One of the most important human pathogens is *Staphylococcus aureus*. *Staphylococcus aureus* causes a wide range of infections, including superficial skin abscesses and severe, life-threatening diseases such as bacteremia and necrotizing pneumonia (Tang et al., 2025). It is an extremely resilient organism because of its remarkable adaptability and high genetic versatility. It has been shown to be present as a commensal microbe in approximately 30% of the human population, and on the other hand, it can persist as a devastating opportunistic pathogen when host defenses are compromised. The World Health Organization (WHO, 2017) has classified methicillin-resistant *Staphylococcus aureus* (MRSA) as a high-priority pathogen, and new therapeutic strategies for it must be rapidly discovered and developed. Researchers believe this highlights the growing public health crisis caused by antibiotic resistance and the critical need for alternative antimicrobial interventions. In addition to its strong antibiotic resistance, *Staphylococcus aureus* also produces several pathogenic factors. One of these important and specific factors is staphyloxanthin (STX), which is known as a golden carotenoid pigment. One of the functions of STX is to contribute to the distinctive coloration of S. aureus colonies. Another role is to provide antioxidant protection to enhance bacterial survival against oxidative stress induced by host immune responses (Cheung et al., 2021). In addition, STX has other roles, including modulating bacterial interactions with host tissues through its redox-active nature, maintaining membrane integrity under stress conditions (Bastos et al., 2025), and stabilizing phage head assembly during viral infection (Touati et al., 2025). Several studies (Detzner et al., 2021; Chatragadda et al., 2021) have reported structural similarities of STX with mammalian cholesterol precursors and suggest that its biosynthetic pathway could serve as a selective drug target without cross-reaction with mammalian sterol metabolism. The synthesis of this pigment is mediated by the highly conserved *crtOPQMN* operon (Wieland et al., 2020). Also, mutants lacking these genes show much lower virulence in animal infection models (Chen et al., 2016; Xue et al., 2019). Therefore, it can be said that there is a direct link between pigment biosynthesis and bacterial pathogenicity. The results of various studies have shown that STX has promising biomedical properties. For example, it has great potential as an adjuvant for antimicrobial therapy (Nguyen et al., 2024) and has significant cytotoxic effects against several human cancer cell lines (Anshi et al., 2024). In addition, one of the multidisciplinary scientific fields that uses a set of tools and techniques derived from engineering, physics, chemistry and biology is the field of nanotechnology (Mohammadabadi et al., 2009; Heydarpour et al., 2011; Mohammadabadi and Mozaffari, 2018). The use of nanotechnology has enabled us to identify submicron bioactive carriers. It has been shown that particle size has a direct impact on the delivery of bioactive substances to target sites in the body and their release behavior (Mortazavi et al., 2005; Zarrabi et al., 2020). The advantages of nanocarriers compared to micrometric carriers include providing more surface area by nanocarriers, increasing solubility potential, increasing bioavailability, improving controlled release and the possibility of precise targeting of entrapped substances (Heydarpour et al., 2011; Mohammadabadi and Mozaffari, 2019). Also, advances in nanotechnology have led to the identification and introduction of innovative strategies to combat microbial infections. One of these is silver nanoparticles (AgNPs). These nanoparticles are potent antimicrobial agents because they have broad-spectrum activity and multimodal mechanisms of action (Jangid et al., 2024). The effects of AgNPs are mainly exerted by disrupting the bacterial cell membrane, interfering with intracellular metabolism, and inducing reactive oxygen species (ROS), while generally maintaining acceptable biocompatibility with mammalian cells (Mette et al., 2022). One of the environmentally friendly and sustainable alternatives to chemical synthesis is the biogenic synthesis of silver nanoparticles using microbial extracts, as it produces nanoparticles with increased stability, targeted activity, and reduced cytotoxicity (Mughal et al., 2021; Khanna et al., 2023). The integration of nanoparticle technology with staphyloxanthin biochemistry has introduced a new approach that can have synergistic therapeutic effects. STX can enhance the bactericidal efficiency of silver nanoparticles by stiffening the membrane (Allahverdiyev et al., 2021). On the other hand, ROS generated by silver nanoparticles may destabilize the antioxidant defense of bacteria, reducing STX and increasing susceptibility (Múnera-Jaramillo et al., 2024). Recent studies have reported STX-mediated modulation of membrane stiffness (Chen et al., 2015) and concluded that nanoparticle interactions can be used to optimize intracellular transport. In addition to the antimicrobial applications of the STX-AgNP complex, it can be used in oncology research and shows selective cytotoxicity towards malignant cells without damaging normal tissues (He et al., 2024). This reduction in damage could be due to differences in cellular uptake and redox metabolism (Du et al., 2011). The STX-AgNP combination has both antimicrobial and anticancer activities, making it a versatile therapeutic platform. Therefore, this dual function can be used for the treatment and control of immunocompromised cancer patients who are at high risk of opportunistic S. aureus infections (Ventola, 2015). Therefore, the aim of the present study was to characterize the biochemical properties of purified STX, optimize the synthesis of biogenic AgNP using S. aureus extracts, and evaluate their combined effects against pathogenic bacteria and human cancer cell lines. The aim of this study was to conduct a thorough investigation of the physicochemical and biological interactions between STX and AgNPs using advanced analytical and imaging techniques, including high-performance liquid chromatography (HPLC) and gas chromatography-mass spectrometry (GC-MS) for pigment analysis, as well as spectroscopic and electron microscopy methods for nanoparticle characterization, and to employ combination index modeling to quantitatively assess therapeutic synergy. More specific goals include elucidating the molecular mechanisms underlying STX-AgNP interactions, contributing to the growing field of hybrid antimicrobial nanomaterials in cancer therapy, uncovering the fundamentals of STX biology, and providing an innovative framework for translating microbial biochemistry into multifunctional therapeutic nanoplatforms.

**Materials and Methods**

**Sample collection and bacterial culture:** The number of clinical specimens used in this study was 221 cases of wound infection, mastitis, and otitis media, of which 137 were human and 84 were animal. To ensure microbial viability, Amies medium was used for processing within two hours of collection. To prepare bacterial cultures, the respective culture media were first dissolved in distilled water, then sterilized using a microwave oven, and finally transferred to sterile Petri dishes. Under standard aseptic conditions, primary isolation and cultivation were performed. Conventional biochemical assays, including catalase and oxidase tests, were used to identify potential colonies of *Staphylococcus aureus*. The Vitek® 2 Compact automated identification system (BioMérieux, France) was used for their confirmation.

**Molecular detection and PCR analysis:** The Presto™ Mini gDNA Bacteria Kit (Geneaid, Taiwan) based on the protocol of the manufacturer was used to extract DNA from the confirmed *S. aureus* isolates. For resuspension and lysis of bacterial pellets GT buffer was used. Then, they were treated by GB buffer and ethanol. For DNA binding and purification, the lysates were transferred onto GD columns. A NanoDrop™ Lite spectrophotometer (Thermo Scientific, USA) was used to assess the quality and concentration of the extracted DNA by calculation of absorbance at 260/280 nm. A GoTaq® Green PCR Master Mix (Promega, USA) in a T100™ Thermal Cycler (Bio-Rad, USA) was used to perform Polymerase chain reaction (PCR). The final volume of each tube was 25 µL. The ingredients of this reaction mixture were 12.5 µL of 2X Master Mix, 5 µL of DNA template (5-50 ng), 3.5 µL of nuclease-free water, and 2 µL of each forward and reverse primer (10 pmol) (Table 1). The thermal cycle used consisted of the following steps: Initial denaturation at 95 °C for 5 min; then 35 cycles, including denaturation at 95 °C for 30 s, annealing at 58 °C for 30 s, synthesis at 72 °C for 1 min; after that final extension at 72 °C for 5 min; and finally hold at 4 °C. The electrophoresis on a 2% agarose gel containing ethidium bromide was used to analyze the PCR products. 0.5X TBE buffer at 100 V for 1 hour was used for running gels. A gel documentation system using ultraviolet transillumination was applied for visualization.

**Staphyloxanthin pigment extraction and purification:** *Staphylococcus aureus* cultures were grown on milk salt agar plates for 72 hours at 37 °C to extract Staphyloxanthin pigment. Bacterial cell harvest was performed after incubation by washing the agar surface with sterile distilled water (3 ml per plate). The suspension was then centrifuged for 15 min at 6000 rpm. Sterile distilled water was used to wash the pellet. Centrifugation was repeated and finally resuspended in 8 ml of 99.9% methanol. All extraction steps were performed under low light and the methanol suspension was wrapped in aluminum foil to minimize light-induced degradation.

**Table 1. Characterizations of used primers for amplification of staphyloxanthin biosynthesis genes applied in this study**

| Target gene | Primer sequence (5′→3′) | PCR product Size (bp) | Accession number |
|---|---|---|---|
| ***crtO*-F** | TGAGAAGCATGGAAAATTTTGGA | 311 | AP023034.1 |
| ***crtO*-R** | ACTGCGTTAATCTCGGTCGA | | |
| ***crtP*-F** | CTTGGAAAAGCTAGCGCGTG | 412 | AP017922.1 |
| ***crtP*-R** | TACTGGCGCTTGTGTGTGAT | | |
| ***crtQ*-F** | GCTGACGGCAAATGGTATGG | 629 | AP040133.1 |
| ***crtQ*-R** | TTTCCTACAGACATTTGGCGA | | |
| ***crtM*-F** | TCATGATGGCGCTTCAGCAT | 517 | AP023034.1 |
| ***crtM*-R** | GCCTGTCTCACTTCGTCCAG | | |
| ***crtN*-F** | GTAGGCGGGCGTATGAATCA | 254 | AP023034.1 |
| ***crtN*-R** | CCATGCGTTGAACCAGGTTC | | |

The suspension was incubated in a water bath at 55 °C for 5 min. It was then allowed to cool at room temperature for 10 min. The supernatant containing the pigment was collected by centrifugation (6000 rpm, 15 min). This process was repeated several times until a colorless cell pellet was obtained and it was ensured that the pigment was completely removed. A UV-Visible spectrophotometer (Thermo Scientific, USA) was used to measure the absorbance of the pooled methanolic extracts at 450 nm for assessment the quantity of pigment concentration. A preparative high-performance liquid chromatography (HPLC) based on a Knauer system (Germany) equipped with an Alltima C18 column (5 µm, 250 × 10 mm) was used to purify the crude pigment extract. The mobile phase had 3 solvents including Solvent A; HPLC-grade water (25% initial, 40% final), Solvent B; Acetonitrile (5% initial, 0% final), and Solvent C; Methanol (70% initial, 60% final). Gradient elution was done at a flow rate of 3 mL/min for 10 minutes. After that, a 2 mL sample was injected via an 8-port valve. Then fractions were collected applying a Foxy R1 fraction collector. A UVD 2.1S detector was used to detect pigment at 450 nm. Based on retention time, area, and purity the chromatographic peaks were analyzed. A rotary evaporator was used for concentrating of purified staphyloxanthin fractions under reduced pressure. Then, they were stored at −20 °C until further biochemical and antioxidant analyses.

**Biogenic silver nanoparticle synthesis and characterization:** A green biological method was used to synthesize biogenic silver nanoparticles (AgNPs). For this, cell-free extract of *Escherichia coli* was prepared by culturing cells in Luria-Bertani (LB) broth. Then, centrifugation at 10,000 × *g* for 10 minutes at 4 °C was performed. After that, to obtain a sterile extract the supernatant was filtered through a 0.22 µm membrane filter. For nanoparticle synthesis, the cell-free extract was mixed with an aqueous 1 mM $AgNO_3$ solution to achieve a final silver ion concentration of 0.1 mM. The reaction mixture was incubated at 37 °C with shaking (150 rpm) for 24 hours. A color change from pale yellow to brown indicated that silver nanoparticles had formed. The synthesized nanoparticles were harvested by centrifugation at 15,000 × g for 20 min. The harvested product was then washed three times with deionized water to remove residual biological material. They were then air-dried. To confirm that nanoparticles were formed and to investigate their properties, the following was performed. A UV-visible spectroscopy was used to record the absorption spectra between 300 and 700 nm and to confirm the surface plasmon resonance characteristic of AgNPs (Figure 1). Then a transmission electron microscopy (TEM) was used to perform morphological and size analysis of AgNPs and to determine nanoparticle shape and distribution (Figure 1) a TEM operation at 120 kV was used. After that, fourier transform infrared spectroscopy (FTIR) was used to obtaine the spectra in the range of 400-4000 $cm^{-1}$ to identify functional groups responsible for nanoparticle stabilization and capping (Figure 2). At the end, X-ray diffraction (XRD) system equipped with Cu Kα radiation (λ = 1.5406 Å), scanning over a 2θ range of 20-80° was used to identify crystallinity and phase (Figure 3).

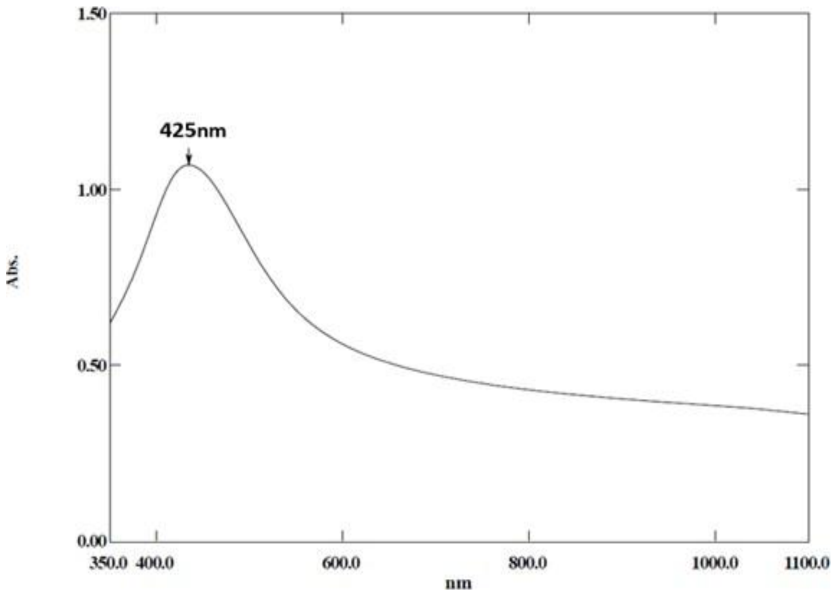


**Figure 1. Nanoparticle morphology and structure obtained from UV-Visible spectral analysis curve of silver nanoparticles (AgNPs) and TEM micrographs**

**Anticancer cytotoxicity assay:** The MTT colorimetric assay was used to evaluate the cytotoxic potential of staphyloxanthin (STX), biogenic silver nanoparticles (AgNPs), and their combination (STX-AgNPs) against three human cancer cell lines: HeLa (cervical adenocarcinoma), MCF-7 (breast adenocarcinoma), and A549 (lung carcinoma). Under standard culture conditions, all cell lines were maintained in their respective media. Dulbecco's Modified Eagle Medium (DMEM) was used for growing HeLa and A549 cells, while Eagle's Minimum Essential Medium (EMEM) was applied for culturing MCF-7 cells. Supplementation of each medium was performed with 10% fetal bovine serum (FBS) and 1% penicillin-streptomycin. Incubation of cultures was done at 37 °C in a humidified atmosphere containing 5% $CO_2$.

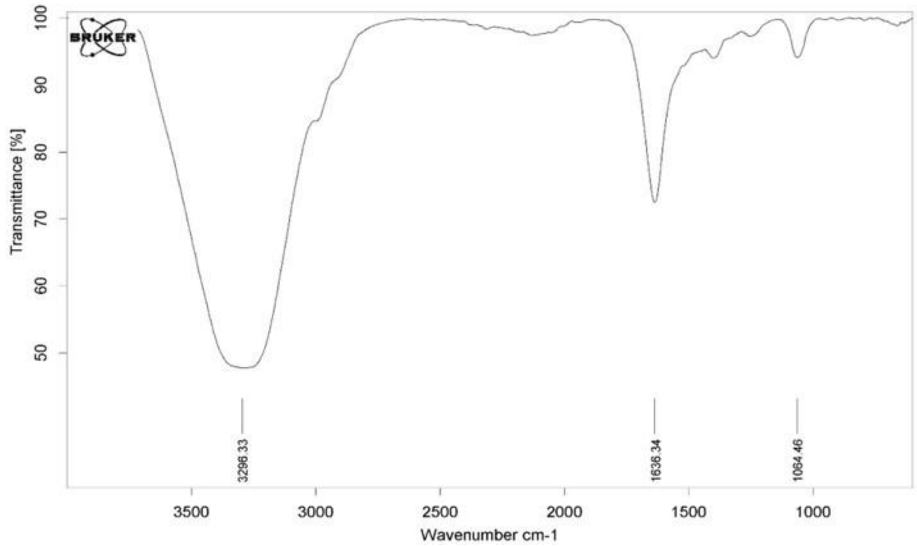


**Figure 2. Spectrum of biogenic silver nanoparticles (AgNPs) using fourier transform infrared (FTIR) in this study**

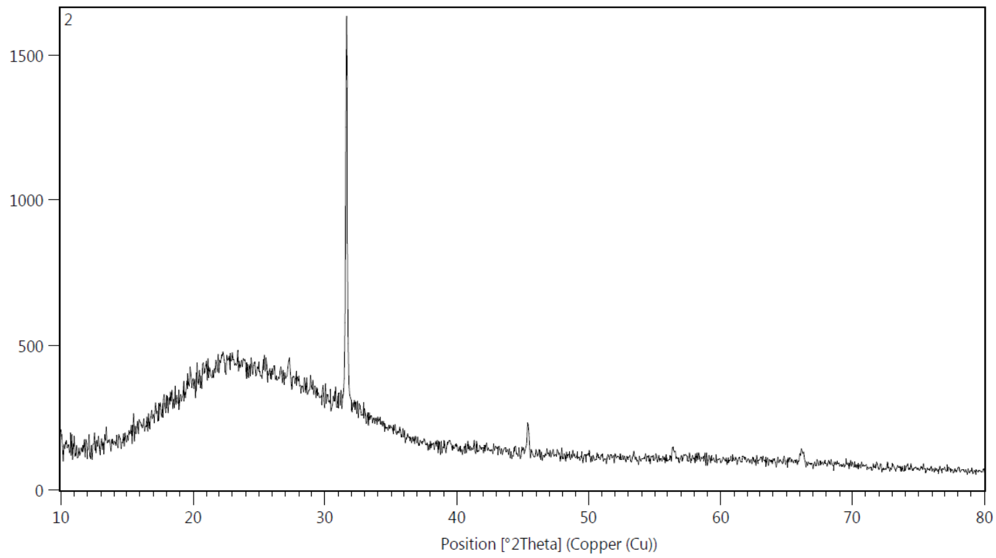


**Figure 3. Crystalline nature of biogenic silver nanoparticles (AgNPs) obtained by X-ray diffraction (XRD) pattern in the present study**

Cells were seeded into 96-well plates at optimized densities of $5 \times 10^3$ cells/well (HeLa), $7 \times 10^3$ cells/well (MCF-7), and $6 \times 10^3$ cells/well (A549), and allowed to adhere for 24 hours to evaluate their cytotoxicity. The cells were then treated with enhancing concentrations (10-320 µg/mL) of STX, AgNPs, or STX-AgNP combinations. Used negative controls were untreated cells. After 24 and 48 hours of incubation, to each well was added 20 µL of MTT solution (5 mg/mL in phosphate-buffered saline). Then, plates were incubated for an additional 4 hours at 37 °C. The supernatant was carefully removed after incubation. Then, 150 µL of dimethyl sulfoxide (DMSO) was added to dissolve the formazan crystals formed by the living cells. A microplate reader (BioTek, USA) was used to measure the optical density at a wavelength of 570 nm. The percentage of cell viability (%) was calculated compared to the untreated control group. Then, using dose-response curves for each treatment group and cell line, the half-maximal inhibitory concentration ($IC_{50}$) values were recorded. Three replicates were considered for each assay. Finally, the results were reported as mean ± standard deviation (SD).

**Statistical analysis:** One-way analysis of variance (ANOVA) followed by Dunnett's post hoc test was used to assess statistical significance between the treatment and control groups. A p value of less than 0.05 was considered statistically significant.

**Results**

**Phenotypic investigation of Staphyloxanthin:** Milk Salt Agar (MSA) was used to evaluate the ability of Staphylococcus aureus isolates to produce the golden yellow carotenoid pigment staphyloxanthin. The isolates were cultured for 24-48 h at 37°C, and colony pigmentation was assessed visually. After washing the colonies with methanol, the intensity of yellow pigmentation was graded on a scale of 0-3, where 0 indicated no pigmentation and 3 indicated intense pigmentation. Different degrees of yellow pigmentation were observed for Staphylococcus aureus isolates on MSA plates. Intense golden yellow color (grade 3) was observed in most isolates (15; 75%). Moderate pigmentation (grade 2) was observed in approximately 20% of isolates. Finally, pale yellow (grade 1) was observed for only 5%. The percentage of completely depigmented isolates (grade 0) was zero. These results indicate that staphyloxanthin production is a common phenotypic feature among *S. aureus* isolates. Differences in the regulatory control or enzymatic efficiency of the carotenoid biosynthetic pathway among isolates could account for the variations in pigmentation intensity.

**Molecular identification of the Staphyloxanthin operon:** Because key genes in the carotenoid biosynthesis operon; *crtO*, *crtP*, *crtQ*, *crtM*, and *crtN* encode essential enzymes responsible for the sequential steps of staphyloxanthin synthesis and are important determinants of pigment production and virulence in *S. aureus*, PCR followed by agarose gel electrophoresis was used to elucidate the genetic basis of staphyloxanthin biosynthesis in eight S. aureus isolates (known as S1-S8). Since distinct amplicons corresponding to each target gene were successfully amplified from all eight isolates, it can be confirmed that they all have the genetic potential for staphyloxanthin synthesis. The sizes of the PCR amplified products on gel electrophoresis were 311 bp (*crtO*), 412 bp (*crtP*), 629 bp (*crtQ*), 517 bp (*crtM*) and 254 bp (*crtN*). This indicates the presence of the entire operon in each strain. These results indicated that these genes have a conserved role in staphyloxanthin biosynthesis in all isolates tested. It was also determined that the differences in the intensity of pigmentation among isolates were due to differences in gene expression levels, differences in gene regulation, or post-translational differences between genes, rather than the absence of the gene. Further studies are needed to compare the expression of these biosynthetic genes among clinical and environmental isolates and the impact of these changes on virulence and resistance to oxidative stress. Figure 4 shows PCR amplification patterns for the *crtM*, *crtN*, *crtP*, and *crtO* genes and Figure 5 represents the *crtQ* gene amplification pattern studied in this research.

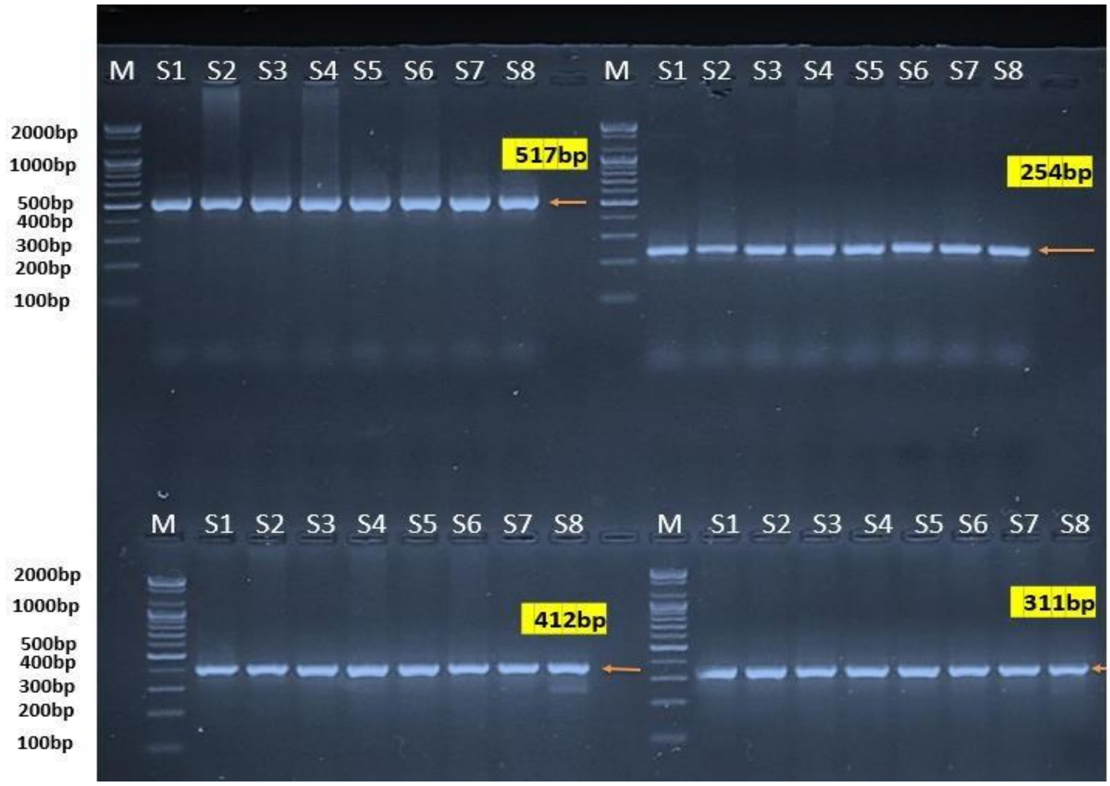


**Figure 4. PCR products o staphyloxanthin biosynthetic operon genes (*crtM*, *crtN*, *crtP*, and *crtO*) in *Staphylococcus aureus* isolates S1-S8 electrophoresed in agarose gel. M is DNA ladder (M100). Lanes S1-S8 are amplification bands for these studied genes with 517 bp, 254 bp, 412 bp, and 311 bp, respectively**

**HPLC purification of Staphyloxanthin:** Preparative high-performance liquid chromatography (HPLC) with an Alltima C18 column (5 µm, 250 × 10 mm) was used to purify staphyloxanthin, a carotenoid pigment. The HPLC system equipment consisted of a triplex pump, an 8-port injection valve, a UV detector, and a fraction collector. Purification was performed using the “staphyloxanthin pigment” method and a 10-min gradient elution program at a flow rate of 3 mL/min. The mobile phase gradient ranged from 5% to 70% and back to 0%, and a UV detector was used to detect the pigment at 450 nm. Fractions corresponding to the staphyloxanthin peak were collected. The system was monitored for pressure, flow rate, and gradient stability during the run. HPLC analysis showed a single, clear peak at a retention time of 8.12 to 8.23 minutes, indicating that the purification of staphyloxanthin was successful. The total area under the peak ranged from 28035.9 to 639700.9 milliampere-hours (mAU) and the peak heights ranged from 0.256 to 14.723 astronomical units (AU).

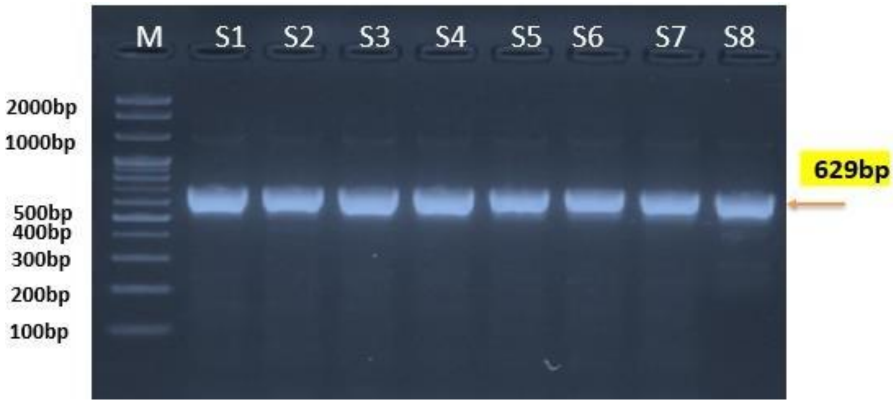


**Figure 5. PCR products o staphyloxanthin biosynthetic operon *crtQ* genes in *Staphylococcus aureus* isolates S1-S8 electrophoresed in agarose gel. M is DNA ladder (M100). Lanes S1-S8 are amplification bands for the *crtQ* gene with 629 bp**

**Antioxidant activity of Staphyloxanthin:** The DPPH (2,2-diphenyl-1-picrylhydrazyl) assay was used to evaluate the free radical scavenging activity of purified staphyloxanthin. The antioxidant activity was high in staphyloxanthin, showing a significant increase in radical scavenging activity, approaching the activity of ascorbic acid (100% at equivalent concentrations). That is, radical scavenging increased from approximately 30% at 10 µg/mL to 86% at 320 µg/mL. Their average optical density (O.D.) and scavenging activity were 10 µg/mL: O.D. 0.237, 29% inhibition; 20 µg/mL: O.D. 0.191, 36% inhibition; 40 µg/mL: O.D. 0.141, 48% inhibition; 80 µg/mL: O.D. 0.130, 53% inhibition; 160 µg/mL: O.D. 0.100, 68% inhibition; and 320 µg/mL: O.D. 0.080, 86% inhibition. While, the ascorbic acid control showed O.D. 0.068, displayed 100% radical scavenging.

**Biosynthesis and characterization of biogenic silver nanoparticles (AgNPs):** Cell-free extracts from pathogenic *Staphylococcus aureus* isolates were used to synthesize biogenic silver nanoparticles. The UV-Visible spectroscopy was applied for confirmation of nanoparticle and showed a characteristic surface plasmon resonance (SPR) peak at 425 nm with an absorbance of

0.763 ± 0.08 AU. The concentration of AgNPs was estimated 55.6 ± 2.1 µg/mL that shows the formation of nanoparticle is efficient. The assessment of nanoparticle size and morphology was done using transmission electron microscopy (TEM). The shape of the silver nanoparticles in TEM images (Figure 6, panels A to F) showed that they were mostly spherical with a narrow size distribution, ranging in size from approximately 23.06 nm to 40.12 nm. The morphology of the stable particles was obtained at different magnifications in the range of 1 to 10 µm; Panel A: TEM distribution at 100 nm; Panel B: TEM distribution at 200 nm; Panel C: TEM distribution at 500 nm; Panel D: TEM distribution at 10 µm; Panel E: TEM distribution at 5 µm; Panel F: TEM distribution at 1 µm.

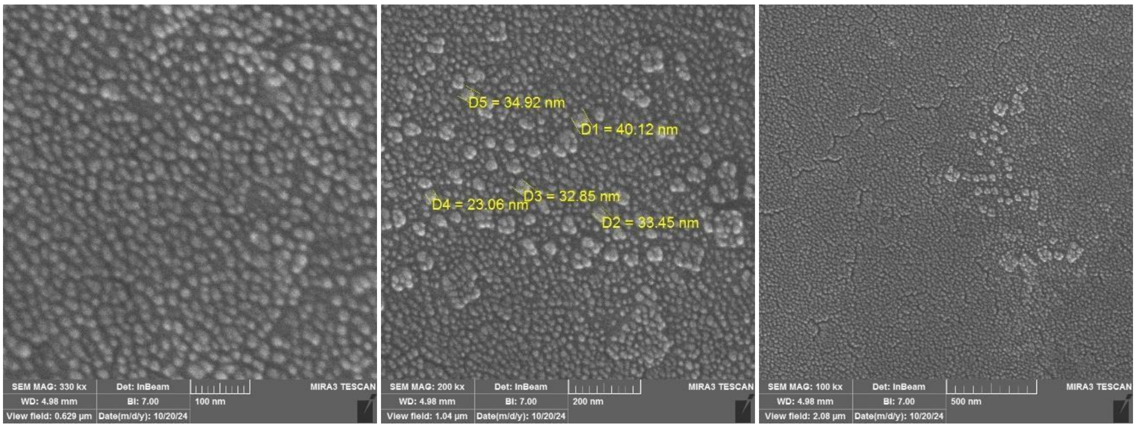


**A: The TEM distribution of (AgNPs) in 100nm.** **B: The TEM distribution of (AgNPs) in 200nm.** **C: The TEM distribution of (AgNPs) in 500nm.**

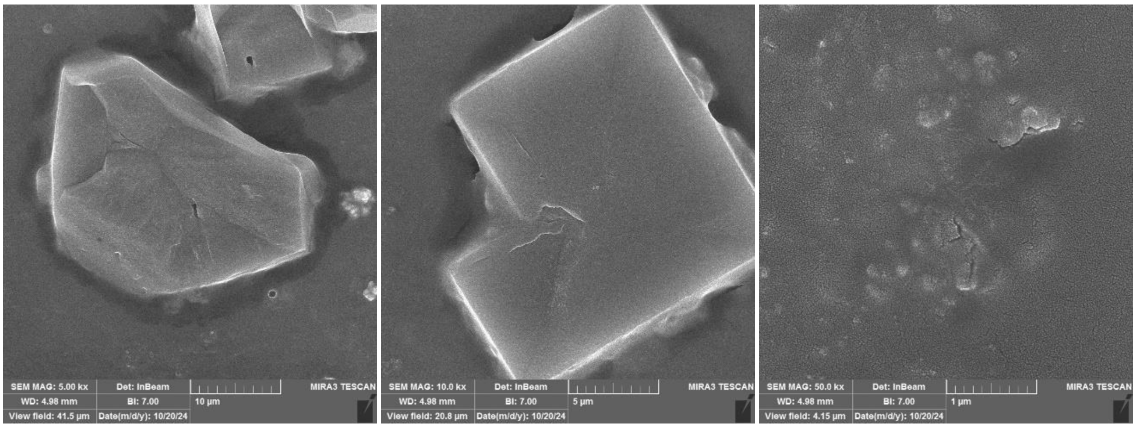

**D: The TEM distribution of (AgNPs) in 10µm.** **E: The TEM distribution of (AgNPs) in 5µm.** **F: The TEM distribution of (AgNPs) in 1µm.**

**Figure 6. Structure and morphology of biogenic silver nanoparticles (AgNPs) synthesized using cell-free extracts of *Staphylococcus aureus* in this study in TEM images**

**Fourier transform infrared (FTIR) spectroscopy of AgNPs:** For analyzing the chemical composition and surface functional groups of biogenic silver nanoparticles (AgNPs), FTIR spectroscopy was used. The spectrum was recorded in the wavenumber range of 3500 to 1000 cm2, where the y-axis represents the transmission percentage (%) and the x-axis represents the wavenumber (cm2). The vibrational modes of the functional groups on the surface of the nanoparticles showed several distinct peaks. Some key findings were: O-H stretching vibrations, indicative of hydroxyl groups or adsorbed water on the AgNP surface, common in aqueous or biosynthesized nanoparticles = ~3208 $cm^{-1}$; C=O stretching (carbonyl groups) or N-H bending (amine groups), likely derived from organic capping agents such as proteins or polyphenols = ~1605 $cm^{-1}$; and C-O stretching vibrations, characteristic of alcohols, ethers, or polysaccharides, supporting the presence of stabilizing biomolecules = ~1064 $cm^{-1}$. The obtained results show that the silver nanoparticles are coated with organic molecules and can act as both capping and stabilizing agents to prevent aggregation. By comparing these capping moieties with known functional groups, their exact nature can be identified. It is believed that this probably originates from biomolecules present in the bacterial extract used to synthesize the nanoparticles.

**X-ray diffraction (XRD) analysis of AgNPs:** For evaluation of the crystallinity, the AgNPs XRD analysis was used. One of the characteristics of crystalline materials is sharp peaks, and in this study, the diffraction pattern showed sharp peaks. The peak at $2\theta = 31.6362°$ was associated with the (111) plane of the face-centered cubic (FCC) silver structure, confirming the formation of crystalline metal nanoparticles. The full width at half maximum (FWHM) of this peak was 0.1476°. This indicates that the particle size is relatively small, consistent with the TEM measurements. Overall, the XRD analysis confirmed the successful synthesis of crystalline silver nanoparticles.

**Anticancer activity and cell line response:** The MTT assay against HeLa (cervical cancer), MCF7 (breast cancer), and CHO (non-cancerous control) cell lines was used to evaluate the anticancer effects of staphyloxanthin (STX), silver nanoparticles (AgNPs), and their combination (STX-AgNPs). Dose-dependent inhibition of cell viability was observed in all treatments. When STX was used alone, the highest concentration (320 µg/mL) resulted in 85% inhibition in HeLa cells and 75% inhibition in MCF7 cells. However, CHO cells showed less sensitivity (45% inhibition). A similar trend was observed for AgNPs. For HeLa cells, 90% inhibition was observed at a concentration of 320 µg/mL, but for CHO cells, 50% inhibition was observed. Complete inhibition (100%) in HeLa cells was achieved with the combination treatment (STX-AgNPs) at a concentration of 320 µg/mL. Values ranging from 0.4 to 0.7 were obtained for the combination index (CI), which could indicate its strong synergistic effects. The IC50 values, i.e. 18.5 µg/mL (HeLa), 28.3 µg/mL (MCF7), and 65.2 µg/mL (CHO), which are evidence of 2.1- to 2.3-fold potency compared to the individual treatments (Figure 7), indicate that the combination treatment is much more potent. Statistical analysis showed that there were significant differences in sensitivity between cancerous and non-cancerous cells ($p < 0.001$). This highlights the selective cytotoxicity of the combination treatment towards malignant cells. The results show that STX-AgNPs have superior anticancer activity with prominent synergistic and selectivity effects on cancer cells.

**Table 2. Some anticancer activity of Staphyloxanthin (STX) measured in this study**

| Concentration (µg/mL) | Inhibition (%) | p-values (vs CHO Control) |
|---|---|---|
| | HeLa | MCF7 |
| 10 | 8.0 ± 1.0 | 6.0 ± 0.9 |
| 20 | 15.0 ± 1.5 | 12.0 ± 1.3 |
| 40 | 30.0 ± 2.0 | 25.0 ± 1.8 |
| 80 | 60.0 ± 2.3 | 50.0 ± 2.1 |
| 160 | 75.0 ± 2.6 | 65.0 ± 2.4 |
| 320 | 85.0 ± 2.9 | 75.0 ± 2.7 |

**Anticancer cytotoxicity and statistical analysis:** The MTT assay was used to evaluate the cytotoxic effects of staphyloxanthin (STX), silver nanoparticles (AgNPs), and their combination (STX-AgNPs) against HeLa (cervical cancer), MCF7 (breast cancer), and CHO (non-cancerous control) cell lines. Dose-dependent inhibition of cell viability was observed in all treatments, indicating that the combination treatment had the strongest effects.

**STX treatment:** STX alone was able to inhibit cancer cell viability in a concentration-dependent manner. Table 2 shows that at a concentration of 320 µg/mL, it showed 85% and 75% inhibition for HeLa and MCF7 cells, respectively, but 45% inhibition was observed for CHO cells. A significant treatment × cell line interaction was observed in the two-way ANOVA ($F(5,12) = 38.94$, $p < 0.0001$). Dunnett's post hoc test showed significant inhibition compared to CHO at concentrations ≥10 µg/ml for HeLa and ≥20 µg/ml for MCF7. The results of relative sensitivity analysis in this study showed that HeLa cells were 2.1 to 2.8 times more sensitive than CHO ($p < 0.01$) and MCF7 cells were 1.6 to 2.2 times more sensitive ($p < 0.05$).

**AgNPs treatment:** Strong anticancer activity was also shown by AgNPs. As table 3 shows, HeLa cells reached 90% inhibition, MCF7 80%, and CHO 50% at 320 µg/mL. A significant treatment effect ($F(5,12) = 52.67$, $p < 0.0001$), with Dunnett's test showing significant inhibition relative to CHO at ≥10 µg/mL for HeLa and ≥20 µg/mL for MCF7 was confirmed by statistical analysis. Relative sensitivity ratios were 2.3-3.1× for HeLa vs CHO and 1.8-2.5× for MCF7 vs CHO. $IC_{50}$ ratios were 0.38 (HeLa/CHO) and 0.52 (MCF7/CHO). These results indicate that cytotoxicity is selective towards cancer cells.

**STX-AgNP combination treatment:** The highest potency and synergy was observed for the combination of STX and AgNPs, with complete inhibition of HeLa cells at a concentration of

320 µg/ml, with 95% inhibition of MCF7 cells and 60% inhibition of CHO cells (Table 4). Two-way ANOVA showed a significant treatment × cell line interaction ($F(2,30) = 36.28$, $p < 0.0001$). Synergy analysis showed combination index (CI) values of 0.4-0.7 at different concentrations, indicating strong synergistic effects ($p < 0.01$). Dose reduction index analysis showed a 3.2-4.5-fold reduction in the dose required for equivalent efficacy compared to single treatments. The sensitivity ratio was 3.1-4.2-fold for HeLa/CHO and 2.5-3.3-fold for MCF7/CHO ($p < 0.001$ for concentrations ≥40 µg/mL). Comparative $IC_{50}$ analysis showed that the combination treatment was more effective and was 18.5 µg/mL for HeLa, 28.3 µg/mL for MCF7, and 65.2 µg/mL for CHO (Figure 7). These results indicate that the STX-AgNP combination has higher anticancer activity and selectivity and can be introduced as a potential synergistic therapy.

**Table 3. Some anticancer activity of AgNPs measured in this study**

| **Concentration (µg/mL)** | **Inhibition (%)** | | **p-values (vs CHO Control)** | |
|---|---|---|---|---|
| | HeLa | MCF7 | CHO | HeLa |
| 10 | 10.0 ± 1.1 | 7.0 ± 1.0 | 3.0 ± 0.6 | 0.019* |
| 20 | 18.0 ± 1.6 | 15.0 ± 1.4 | 7.0 ± 0.9 | 0.003** |
| 40 | 35.0 ± 2.1 | 30.0 ± 2.0 | 15.0 ± 1.3 | 0.0002*** |
| 80 | 65.0 ± 2.4 | 55.0 ± 2.2 | 30.0 ± 1.6 | 0.0001*** |
| 160 | 80.0 ± 2.7 | 70.0 ± 2.5 | 40.0 ± 1.9 | 0.0001*** |
| 320 | 90.0 ± 3.0 | 80.0 ± 2.8 | 50.0 ± 2.1 | 0.0001*** |

**Table 4. Some anticancer activity of STX-AgNP combination measured in this study**

| **Concentration (µg/mL)** | **Inhibition (%)** | | **p-values (vs CHO Control)** | |
|---|---|---|---|---|
| | HeLa | MCF7 | CHO | HeLa |
| 10 | 12.0 ± 1.2 | 10.0 ± 1.1 | 5.0 ± 0.7 | 0.017* |
| 20 | 23.0 ± 1.8 | 20.0 ± 1.7 | 10.0 ± 1.0 | 0.002** |
| 40 | 41.0 ± 2.1 | 38.0 ± 2.0 | 20.0 ± 1.4 | 0.0001*** |
| 80 | 80.0 ± 2.5 | 70.0 ± 2.4 | 35.0 ± 1.8 | 0.0001*** |
| 160 | 90.0 ± 2.7 | 85.0 ± 2.6 | 50.0 ± 2.0 | 0.0001*** |
| 320 | 100.0 ± 0.0 | 95.0 ± 2.9 | 60.0 ± 2.3 | 0.0001*** |

## Discussion

The results of this study highlighted that biogenic silver nanoparticles (AgNPs) and staphyloxanthin (STX) have a synergistic potential for cancer treatment and their combination can provide a therapeutic platform against breast (MCF-7) and cervical (HeLa) cancer cell lines. In addition, it showed lower cytotoxicity than non-cancerous CHO cells. STX, a carotenoid pigment produced by *Staphylococcus aureus*, showed dose-dependent cytotoxicity and was successful in inhibiting HeLa and MCF-7 cells by 85% and 75% at 320 µg/mL, respectively. On the other hand, CHO cells showed much lower sensitivity with 45% inhibition. Most likely, the antioxidant properties of STX and its structural similarity to cholesterol precursors, which may disrupt lipid integrity in the membranes of cancer cells, have caused this selective cytotoxicity (Almatroudi, 2024).

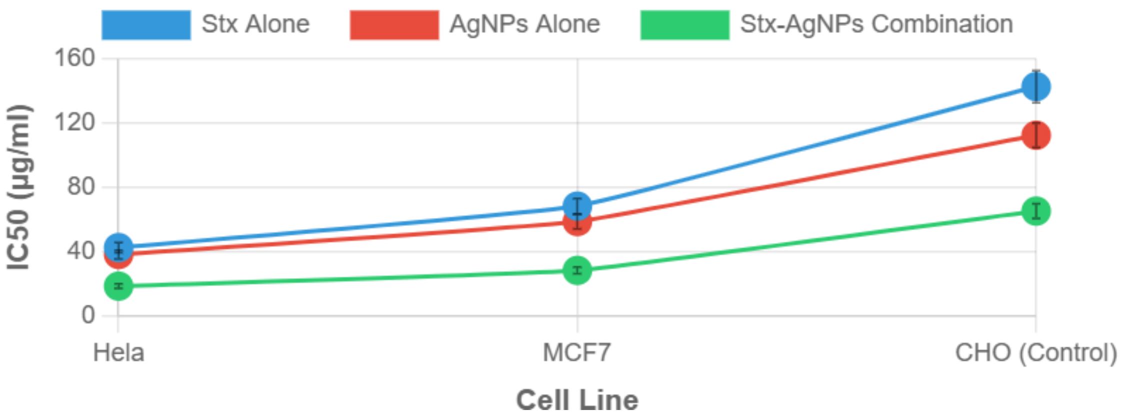


**Figure 7. Comparative $IC_{50}$ analysis across treatments observed in three cell lines assessed in this study**

Biogenic silver nanoparticles synthesized from S. aureus extracts enhanced the anticancer activity and when used at the same concentration, they caused 90% and 80% inhibition in HeLa and MCF-7 cells, respectively. This is probably because they can produce reactive oxygen species (ROS) and induce apoptosis (Durán et al., 2016). Furthermore, the STX-AgNP combination at a concentration of 320 µg/mL resulted in 100% inhibition in HeLa cells and 95% inhibition in MCF-7 cells. Also, the combination index (CI) value was less than 1 (0.4-0.7), confirming strong synergistic interactions (Chou, 2010). For this combination (18.5 µg/ml for HeLa and 28.3 µg/ml for MCF-7), the IC50 values were 2.3-2.4-fold lower than the individual treatments. This highlights the therapeutic advantage of this dual approach. The selectivity index (3.36× for HeLa and 2.09× for MCF-7 versus CHO cells) is more strongly indicative of preferential targeting of malignant cells. This is likely due to different uptake or metabolic vulnerabilities in cancer cells (Zhang et al., 2024). The mechanism of action of these events could be that STX may increase AgNP uptake by modulating membrane fluidity, and AgNPs may enhance the pro-oxidant effects of STX in cancer cells by taking advantage of high oxidative stress (Pandey et al., 2025). The spherical morphology (23.06-40.12 nm) and crystallinity of AgNPs, which are crucial for nanoparticle stability and cellular interactions, have been demonstrated by TEM and XRD analyses (Sati et al., 2025). On the other hand, FTIR identifies organic capping agents that may be effective in improving biocompatibility (Lasmi et al., 2025). Although the potent antioxidant activity of STX (86% DPPH radical scavenging at a concentration of 320 µg/mL) has been demonstrated, it is likely to act as a pro-oxidant in cancer cells and synergize with AgNP-induced

ROS and enhance cytotoxicity (Zhang et al., 2019). Therefore, efforts are currently underway to develop compatible hybrid nanomaterial systems that provide multifunctional platforms to overcome chemoresistance while minimizing off-target effects (Huh & Kwon, 2011). The lack of in vivo validation and detailed investigation of molecular target mechanisms, such as STX interactions with oncogenic pathways (e.g., PI3K/AKT or NF-κB), is a limitation of this study (Hashemi et al., 2024). Future research should consider using targeted drug delivery strategies, such as ligand-bound or stimulus-responsive nanoparticles, to increase specificity (Serri, 2025). Comparative analyses with conventional chemotherapies (such as cisplatin or doxorubicin) should also be used to assess efficacy and safety. Another essential task in the future is to optimize the scalable biogenic AgNP production and purification of STX for industrial and clinical application (Mughal et al., 2021; Khanna et al., 2023). Such research opens new avenues for the repurposing of microbial pigments in oncology, and parallel compounds such as prodigiosin and violacein (Xue et al., 2019; Dang & Guan, 2020; Laraib et al., 2022).

**Conclusion:** From the results of this study, it can be concluded that the STX-AgNP combination can be a promising model in cancer treatment. Because by integrating nanotechnology and microbial biochemistry, it attempts to propose a selective, synergistic, and potentially sustainable therapeutic strategy for cancer treatment. Among the things that strengthen its potential in this direction, we can mention its strong activity against cervical and breast cancer cells, along with reduced cytotoxicity towards normal cells. To confirm the efficacy, clarify the mechanisms of action, and expand its applications across oncology, it is necessary to conduct more preclinical and clinical studies with a wider scope.

**Author contributions**

HKJ and HHN were Conceptualization and methodology, software and validation, formal analysis and investigation, resources, data curation, writing-original draft preparation, writing review, visualization, and funding acquisition.

**Data availability statement**

Data are available from the authors upon reasonable request.

**Acknowledgements**

The authors thank all staff of molecular biology department, college of veterinary medicine, Al-qadisya university for helping to complete this research.

**Ethical considerations**

The research was confirmed by the ethical standards of the University of Al-Qadisiyah, Iraq, and in compliance with the principles of the Declaration of Helsinki. Ethical approval was granted under reference number 42-11/10/2014. Written informed consent was achieved from all participants or their legal guardians prior to specimen collection. All procedures also complied with institutional animal care and use committee (IACUC) guidelines

**Funding**

No external funding was received for this study from public, commercial, or charitable organizations.

**Conflict of interest**

The author declared no conflict interest related to this paper.

**References**

Allahverdiyev, A. M., Kon, K. V., Abamor, E. S., Bagirova, M., & Rafailovich, M. (2011). Coping with antibiotic resistance: Combining nanoparticles with antibiotics and other antimicrobial agents. *Expert Review of Anti-Infective Therapy*, *9*(11), 1035-1052. https://doi.org/10.1586/eri.11.121

Almatroudi, A. (2024). Unlocking the potential of silver nanoparticles: From synthesis to versatile bio-applications. *Pharmaceutics*, *16*(9), Article 1232. https://doi.org/10.3390/pharmaceutics16091232

Anshi, Kapil, S., Goswami, L., & Sharma, V. (2024). Unveiling the intricacies of microbial pigments as sustainable alternatives to synthetic colorants: Recent trends and advancements. *Micro*, *4*(4), 621-640. https://doi.org/10.3390/micro4040038

Bastos, M. L. C., Ferreira, G. G., Kosmiscky, I. O., Guedes, I. M. L., Muniz, J. A. P. C., Carneiro, L. A., Peralta, Í. L. C., Bahia, M. N. M., Souza, C. O., & Dolabela, M. F. (2025). What do we know about *Staphylococcus aureus* and oxidative stress? Resistance, virulence, new targets, and therapeutic alternatives. *Toxics*, *13*(5), Article 390. https://doi.org/10.3390/toxics13050390

Chatragadda, R., & Dufossé, L. (2021). Ecological and biotechnological aspects of pigmented microbes: A way forward in development of food and pharmaceutical grade pigments. *Microorganisms*, *9*(3), Article 637. https://doi.org/10.3390/microorganisms9030637

Chen, F., Di, H., Wang, Y., Cao, Q., Xu, B., Zhang, X., Yang, N., Liu, G., Yang, C. G., Xu, Y., Jiang, H., Lian, F., Zhang, N., Li, J., & Lan, L. (2016). Small-molecule targeting of a diapophytoene desaturase inhibits *S. aureus* virulence. *Nature Chemical Biology*, *12*(3), 174-179. https://doi.org/10.1038/nchembio.2003

Chen, Y., Gao, D. Y., & Huang, L. (2015). In vivo delivery of miRNAs for cancer therapy: Challenges and strategies. *Advanced Drug Delivery Reviews*, *81*, 128-141. https://doi.org/10.1016/j.addr.2014.05.009

Cheung, G. Y. C., Bae, J. S., & Otto, M. (2021). Pathogenicity and virulence of *Staphylococcus aureus*. *Virulence*, *12*(1), 547-569. https://doi.org/10.1080/21505594.2021.1878688

Chou, T. C. (2010). Drug combination studies and their synergy quantification using the Chou-Talalay method. *Cancer Research*, *70*(2), 440-446. https://doi.org/10.1158/0008-5472.CAN-09-1947

Dang, Y., & Guan, J. (2020). Nanoparticle-based drug delivery systems for cancer therapy. *Smart Materials in Medicine*, *1*, 10-19. https://doi.org/10.1016/j.smaim.2020.04.001

Detzner, J., Klein, A. L., Pohlentz, G., Krojnewski, E., Humpf, H. U., Mellmann, A., Karch, H., & Müthing, J. (2021). Primary human renal proximal tubular epithelial cells (pHRPTEpiCs): Shiga toxin (Stx) glycosphingolipid receptors, Stx susceptibility, and interaction with membrane microdomains. *Toxins*, *13*(8), Article 529. https://doi.org/10.3390/toxins13080529

Du, J., Shao, Z., & Zhao, H. (2011). Engineering microbial factories for synthesis of value-added products. *Journal of Industrial Microbiology & Biotechnology*, *38*(8), 873-890. https://doi.org/10.1007/s10295-011-0970-3

Durán, N., Durán, M., de Jesus, M. B., Seabra, A. B., Fávaro, W. J., & Nakazato, G. (2016). Silver nanoparticles: A new view on mechanistic aspects on antimicrobial activity. *Nanomedicine: Nanotechnology, Biology, and Medicine*, *12*(3), 789-799. https://doi.org/10.1016/j.nano.2015.11.016

Hashemi, M., Rahimzadeh, P., Koohpar, Z. K., Izadi, H., Karami, A., Bakhtiari Beklar, H., Mahmoudjanlou, A., Atabi, F., Nabavi, N., Farahani, N., Taheriazam, A., Orouei, S., & Entezari, M. (2024). Apoptosis mechanism in cancer: Overview and recent advances. In *Autophagy, apoptosis and ferroptosis in oncology* (pp. 317-377). World Scientific. https://doi.org/10.1142/9789811299322_0011

He, M., Chen, S., Yu, H., Fan, X., Wu, H., Wang, Y., Wang, H., & Yin, X. (2024). Advances in nanoparticle-based radiotherapy for cancer treatment. *iScience*, *28*(1), Article 111602. https://doi.org/10.1016/j.isci.2024.111602

Heidarpour, F., Mohammadabadi, M. R., Zaidul, I. S. M., Maherani, B., Saari, N., Hamid, A. A., Abas, F., Manap, M. Y. A., & Mozafari, M. R. (2011). Use of prebiotics in oral delivery of bioactive compounds: A nanotechnology perspective. *Pharmazie, 66*(5), 319-324. https://doi.org/10.1691/ph.2011.0279

Huh, A. J., & Kwon, Y. J. (2011). "Nanoantibiotics": A new paradigm for treating infectious diseases using nanomaterials in the antibiotics resistant era. *Journal of Controlled Release*, *156*(2), 128-145. https://doi.org/10.1016/j.jconrel.2011.07.002

Jangid, H., Singh, S., Kashyap, P., Singh, A., & Kumar, G. (2024). Advancing biomedical applications: An in-depth analysis of silver nanoparticles in antimicrobial, anticancer, and wound healing roles. *Frontiers in Pharmacology*, *15*, Article 1438227. https://doi.org/10.3389/fphar.2024.1438227

Khanna, K., Kohli, S. K., Bakshi, P., Sharma, P., Kour, J., Bhardwaj, T., Sharma, N., Dogra, N., Ohri, P., Sirhindi, G., & Bhardwaj, R. (2023). Green biosynthesis of nanoparticles: Mechanistic aspects and applications. In P. Singh, V. Kumar, M. Bakshi, C. M. Hussain, & M. Sillanpää (Eds.), *Environmental applications of microbial nanotechnology* (pp. 99-126). Elsevier. https://doi.org/10.1016/B978-0-323-91744-5.00020-5

Laraib, U., Sargazi, S., Rahdar, A., Khatami, M., & Pandey, S. (2022). Nanotechnology-based approaches for effective detection of tumor markers: A comprehensive state-of-the-art review. *International Journal of Biological Macromolecules*, *195*, 356-383. https://doi.org/10.1016/j.ijbiomac.2021.12.052

Lasmi, F., Hamitouche, H., Laribi-Habchi, H., Benguerba, Y., & Chafai, N. (2025). Silver nanoparticles (AgNPs), methods of synthesis, characterization, and their application: A review. *Plasmonics*. Advance online publication. https://doi.org/10.1007/s11468-025-02894-9

Mette, M., Connolly, W., Vishwanath, N., Allu, S., Whitaker, C., Stone, B. K., Antoci, V., Born, C. T., & Garcia, D. R. (2022). Silver carboxylate as an antibiotic-independent antimicrobial: A review of current formulations, *in vitro* efficacy, and clinical relevance. *Medical Research Archives*, *10*(12), Article 3388. https://doi.org/10.18103/mra.v10i12.3388

Mohammadabadi, M. R., & Mozafari, M. R. (2018). Enhanced efficacy and bioavailability of thymoquinone using nanoliposomal dosage form. *Journal of Drug Delivery Science and Technology, 47*(1), 445-453. https://doi.org/10.1016/j.jddst.2018.08.019

Mohammadabadi, M. R., & Mozafari, M. R. (2019). Development of nanoliposome-encapsulated thymoquinone: Evaluation of loading efficiency and particle characterization. *Journal of Biopharmaceuticals, 11*(4), 39-46.

Mohammadabadi, M. R., El-Tamimy, M., Gianello, R., & Mozafari, M. R. (2009). Supramolecular assemblies of zwitterionic nanoliposome-polynucleotide complexes as gene transfer vectors: Nanolipoplex formulation and *in vitro* characterization. *Journal of Liposome Research, 19*(2), 105-115. https://doi.org/10.1080/08982100802547326.

Mortazavi, S. M., Mohammadabadi, M. R., & Mozafari, M. R. (2005). Applications and *in vivo* behaviour of lipid vesicles. In M. R. Mozafari (Ed.), *Nanoliposomes: From fundamentals to recent developments* (pp. 67-76).

Mughal, B., Zaidi, S. Z. J., Zhang, X., & Hassan, S. U. (2021). Biogenic nanoparticles: Synthesis, characterisation and applications. *Applied Sciences*, *11*(6), Article 2598. https://doi.org/10.3390/app11062598

Múnera-Jaramillo, J., López, G.-D., Suesca, E., Carazzone, C., Leidy, C., & Manrique-Moreno, M. (2024). The role of staphyloxanthin in the regulation of membrane biophysical properties in *Staphylococcus aureus*. *Biochimica et Biophysica Acta (BBA) - Biomembranes*, *1866*(3), Article 184288. https://doi.org/10.1016/j.bbamem.2024.184288

Nguyen, T. T. T., Nguyen, T. T. T., Nguyen, H. D., Nguyen, T. K., Pham, P. T. V., Tran, L. T. T., Pham, H. K. T., Truong, P. C. H., Tran, L. T., & Tran, M. H. (2024). Anti-*Staphylococcus aureus* potential of compounds from *Ganoderma* sp.: A comprehensive molecular docking and simulation approaches. *Heliyon*, *10*(7), Article e28118. https://doi.org/10.1016/j.heliyon.2024.e28118

Pandey, P., Lakhanpal, S., Bishoyi, A. K., Jyothi, S. R., Mishra, S., Verma, M., Singh, A., Alam, M. W., Rab, S. O., Saeed, M., & Khan, F. (2025). Biosynthesis of silver nanoparticles from plant extracts: A comprehensive review focused on anticancer therapy. *Frontiers in Pharmacology*, *16*, Article 1600347. https://doi.org/10.3389/fphar.2025.1600347

Sati, A., Ranade, T. N., Mali, S. N., Ahmad Yasin, H. K., & Pratap, A. (2025). Silver nanoparticles (AgNPs): Comprehensive insights into bio/synthesis, key influencing factors, multifaceted applications, and toxicity—A 2024 update. *ACS Omega*, *10*(8), 7549-7582. https://doi.org/10.1021/acsomega.4c11045

Serri, C. (2025). Editorial on special issue: Advances in nanotechnology-based drug delivery systems. *Pharmaceutics*, *17*(8), Article 1038. https://doi.org/10.3390/pharmaceutics17081038

Tong, S. Y. C., Fowler, V. G., Jr., Skalla, L., & Holland, T. L. (2025). Management of *Staphylococcus aureus* bacteremia: A review. *JAMA*, *334*(9), 798-808. https://doi.org/10.1001/jama.2025.4288

Touati, A., Ibrahim, N. A., & Idres, T. (2025). Disarming *Staphylococcus aureus*: Review of strategies combating this resilient pathogen by targeting its virulence. *Pathogens*, *14*(4), Article 386. https://doi.org/10.3390/pathogens14040386

Ventola, C. L. (2015). The antibiotic resistance crisis: Part 1: Causes and threats. *P & T: A Peer-Reviewed Journal for Formulary Management*, *40*(4), 277-283. https://www.ncbi.nlm.nih.gov/pmc/articles/PMC4378521/

Wieland, B., Feil, C., Gloria-Maercker, E., Thumm, G., Lechner, M., Bravo, J.-M., Poralla, K., & Götz, F. (1994). Genetic and biochemical analyses of the biosynthesis of the yellow carotenoid 4,4′-diaponeurosporene of *Staphylococcus aureus*. *Journal of Bacteriology*, *176*(24), 7719-7726. https://doi.org/10.1128/jb.176.24.7719-7726.1994

World Health Organization. (2017). *Global priority list of antibiotic-resistant bacteria*. https://www.who.int/publications/i/item/WHO-EMP-IAU-2017.12

Xue, L., Chen, Y. Y., Yan, Z., Lu, W., Wan, D., & Zhu, H. (2019). Staphyloxanthin: A potential target for antivirulence therapy. *Infection and Drug Resistance*, *12*, 2151-2160. https://doi.org/10.2147/IDR.S193649

Zarrabi, A., Alipoor Amro Abadi, M., Khorasani, S., Mohammadabadi, M., Jamshidi, A., Torkaman, S., Taghavi, E., Mozafari, M. R., & Rasti, B. (2020). Nanoliposomes and tocosomes as multifunctional nanocarriers for the encapsulation of nutraceutical and dietary molecules. *Molecules, 25*(3), 638. https://doi.org/10.3390/molecules25030638

Zhang, J., Wu, Y., Li, Y., Li, S., Liu, J., Yang, X., Xia, G., & Wang, G. (2024). Natural products and derivatives for breast cancer treatment: From drug discovery to molecular mechanism. *Phytomedicine*, *129*, Article 155600. https://doi.org/10.1016/j.phymed.2024.155600

Zhang, L., Liang, E., Cheng, Y., Mahmood, T., Ge, F., Zhou, K., Bao, Y., Liao, X., & Wang, J. (2020). Is the development of *Staphylococcus aureus* infections linked to virulence factors? *Future Microbiology*, *15*(9), 801-816. https://doi.org/10.2217/fmb-2019-0337

Zhang, Y., Li, M., Gao, X., Chen, Y., & Liu, T. (2019). Nanotechnology in cancer diagnosis: Progress, challenges and opportunities. *Journal of Hematology & Oncology*, *12*(1), Article 137. https://doi.org/10.1186/s13045-019-0833-3

مجله بیوتکنولوژی کشاورزی
انجمن بیوتکنولوژی ایران
دانشگاه شهید باهنر کرمان
شاپا چاپی: ۶۷۰۵-۲۲۲۸ شاپا الکترونیکی: ۶۵۰۰-۲۲۲۸

# کاربرد ترکیب استافیلوگزانتین-نانوذرات نقره به‌عنوان یک بستر درمانی پایدار با پتانسیل ضدسرطانی

**حوراء کریم جودی**

نویسنده مسئول، گروه میکروب‌شناسی، دانشکده دامپزشکی، دانشگاه القادسیه، القادسیه، عراق. ایمیل: hawraa-kareemjudi@gmail.com

**حسن هاشم ناصر**

واحد پژوهشی بیماری‌های قابل‌انتقال بین انسان و حیوان، دانشکده دامپزشکی، دانشگاه القادسیه، القادسیه، عراق. ایمیل: hassan-naser@qu.edu.iq

تاریخ دریافت: ۱۴۰۴/۰۶/۱۹ تاریخ دریافت فایل اصلاح شده نهایی: ۱۴۰۴/۰۸/۱۶ تاریخ پذیرش: ۱۴۰۴/۰۸/۱۷

---

**چکیده**

**هدف:** استافیلوکوکوس اورئوس یکی از پاتوژن‌های اصلی انسانی است که طیف وسیعی از عفونت‌ها را ایجاد می‌کند؛ از بیماری‌های خفیف پوستی گرفته تا عفونت‌های سیستمیک شدید. یک رنگدانه کاروتنوئیدی طلایی به نام استافیلوگزانتین، عامل تعیین‌کننده وایرولانس این باکتری است. این ترکیب به‌عنوان یک آنتی‌اکسیدان عمل کرده و از باکتری در برابر استرس اکسیداتیو محافظت می‌کند. هدف این پژوهش بررسی ویژگی‌های مولکولی و بیوشیمیایی استافیلوگزانتین و نیز ارزیابی نقش و پتانسیل آن در ترکیب با نانوذرات نقره زیستی (AgNPs) برای درمان پایدار و بررسی فعالیت ضدسرطانی آن بود.

**مواد و روش‌ها:** تولید استافیلوگزانتین توسط ایزوله‌های بالینی استافیلوکوکوس اورئوس بر اساس میزان رنگدانه تولیدشده مورد بررسی قرار گرفت. برای تأیید ژنتیکی ژن‌های بیوسنتزی *crtO*، *crtP*، *crtQ*، *crtM*و *crtN* از واکنش زنجیره‌ای پلیمراز (PCR) استفاده شد. تخلیص رنگدانه با کروماتوگرافی مایع با کارایی بالا (HPLC) انجام گرفت. سپس، آزمون مهار رادیکال DPPH برای ارزیابی ظرفیت آنتی‌اکسیدانی آن به‌کار رفت. از عصاره‌های *S. aureus* برای سنتز نانوذرات نقره زیستی استفاده شد. پیک تشدید پلاسمون سطحی در طول‌موج ۴۲۵ نانومتر با استفاده از طیف‌سنجی فرابنفش-مرئی تأیید شد. در ادامه، اثرات سمی سلولی و هم‌افزای استافیلوگزانتین و نانوذرات نقره، به‌صورت جداگانه و ترکیبی، بر روی رده‌های سلولی سرطانی HeLa (دهانه رحم) و MCF-7 (پستان) ارزیابی گردید. سلول‌های CHO به‌عنوان کنترل غیرسرطانی استفاده شدند.

**نتایج:** در ۷۵٪ از ایزوله‌ها رنگدانه‌های طلایی شدیدی مشاهده شد. تمام ژن‌های بیوسنتز استافیلوگزانتین با PCR تأیید شدند. یک

پیک واضح و منفرد با زمان بازداری ۸/۱۲ تا ۸/۲۳ دقیقه و سطح ۲۸۰۳۵/۹ تا ۶۳۹۷۰۰/۹ mA·h در HPLC شناسایی شد. فعالیت آنتی‌اکسیدانی قوی رنگدانه منجر به مهار ۸۶٪ از رادیکال‌های DPPH در غلظت ۳۲۰ میکروگرم بر میلی‌لیتر شد که از نظر شدت با فعالیت اسید آسکوربیک قابل مقایسه بود. غلظت نانوذرات نقره زیستی کروی (۲۳/۰۶–۴۰/۱۲ نانومتر) برابر با ۲/۱± ۵۵/۶ میکروگرم بر میلی‌لیتر بود. درمان ترکیبی استافیلوگزانتین– AgNP اثر سمی وابسته به دوز قوی‌تری بر سلول‌های سرطانی ایجاد کرد و در غلظت ۳۲۰ میکروگرم بر میلی‌لیتر مهار کامل رشد سلولی را به‌همراه داشت، در حالی که سمیت پایینی بر سلول‌های CHO نشان داد. مقادیر شاخص ترکیب (CI < 1) بیانگر هم‌افزایی قوی و افزایش ۲/۱–۳/۵ برابری توان درمان‌های منفرد بود.

**نتیجه‌گیری:** بر اساس نتایج به‌دست‌آمده، می‌توان گفت که کمپلکس استافیلوگزانتین–نانوذرات نقره (STX-AgNP) می‌تواند به‌عنوان یک بستر درمانی نویدبخش و چندمنظوره با فعالیت ضدسرطانی قوی و انتخاب‌گر عمل کند. با توجه به اثرات هم‌افزای چشمگیر و منشأ زیستی آن، این ترکیب می‌تواند در درمان پایدار سرطان و کنترل مقاومت میکروبی کاربرد بالقوه‌ای داشته باشد. بااین‌حال، انجام مطالعات بیشتر در مقیاس وسیع‌تر برای دستیابی به نتایج قطعی ضروری است.

**کلمات کلیدی:** استافیلوگزانتین، فعالیت ضدسرطانی، نانوذرات نقره، *Staphylococcus aureus*

**نوع مقاله**: پژوهشی

**استناد:** حوراء کریم جودی، حسن هاشم ناصر (۱۴۰۴). کاربرد ترکیب استافیلوگزانتین–نانوذرات نقره به‌عنوان یک بستر درمانی پایدار با پتانسیل ضدسرطانی. *مجله بیوتکنولوژی کشاورزی*، ۱۷(۴)، ۴۱۵–۴۳۸.

Publisher: Shahid Bahonar University of Kerman & Iranian Biotechnology Society.